

Please cite the Published Version

Teimouri, Samaneh , Potgieter, Johannes Herman , Billing, Caren  and Conradie, Jeanet 
(2023) The feasibility of pyrite dissolution in the deep eutectic solvent ethaline: experimental and theoretical study. *Journal of Molecular Liquids*, 392. 123468 ISSN 0167-7322

DOI: <https://doi.org/10.1016/j.molliq.2023.123468>

Publisher: Elsevier BV

Version: Published Version

Downloaded from: <https://e-space.mmu.ac.uk/633643/>

Usage rights:  [Creative Commons: Attribution-Noncommercial-No Derivative Works 4.0](https://creativecommons.org/licenses/by-nc-nd/4.0/)

Additional Information: This is an open access article which originally appeared in *Journal of Molecular Liquids*, published by Elsevier

Data Access Statement: The authors do not have permission to share data.

Enquiries:

If you have questions about this document, contact openresearch@mmu.ac.uk. Please include the URL of the record in e-space. If you believe that your, or a third party's rights have been compromised through this document please see our Take Down policy (available from <https://www.mmu.ac.uk/library/using-the-library/policies-and-guidelines>)



The feasibility of pyrite dissolution in the deep eutectic solvent ethaline: Experimental and theoretical study

Samaneh Teimouri^{a,*}, Johannes Herman Potgieter^{a,b}, Caren Billing^c, Jeanet Conradie^d

^a Sustainable and Innovative Minerals and Metals Extraction Technology (SIMMET) group, School of Chemical and Metallurgical Engineering, University of the Witwatersrand, Private Bag X3, Wits 2050, South Africa

^b Department of Natural Science, Manchester Metropolitan University, Chester Street, Manchester M1 5GD, UK

^c Sustainable and Innovative Minerals and Metals Extraction Technology (SIMMET) group, School of Chemistry, University of the Witwatersrand, Private Bag X3, Wits 2050, South Africa

^d Department of Chemistry, University of the Free State, 9300, Nelson Mandela Street, Bloemfontein, South Africa

ARTICLE INFO

Keywords:

Pyrite
Deep eutectic solvent (DES)
Ethaline
Density functional theory (DFT)
Fourier-transform infrared (FTIR) spectroscopy

ABSTRACT

Environmental concerns about the traditional gold extraction process, and the potential volume of encapsulated gold in sulfidic minerals i.e. pyrite, have motivated researchers to find effective, efficient and ecologically benign ways to expose the enclosed gold for improved extraction. Neoteric deep eutectic solvents (DESs) are an analogue of ionic liquids (ILs) which are gaining more attention as eco-friendly solvents. This study examined the viability of pyrite dissolution in a DES comprised of choline chloride (ChCl) and ethylene glycol (EG), called Ethaline. The pH of the ethaline solvent mixed with hydrogen peroxide oxidant, and different solid-to-liquid ratios were examined. Ethaline solution with pH 8 provided the desired condition at which EG is deprotonated to $[\text{C}_2\text{H}_4\text{O}_2]^{2-}$, a favourable ligand for Fe complexation and thus pyrite dissolution. A solid-to-liquid ratio of 1/20 was optimal and achieved 23.6% Fe extraction as an indication of pyrite dissolution. Density functional theory (DFT) was applied to determine which of the two ligands provided by ethaline (Cl^- and/or $[\text{C}_2\text{H}_4\text{O}_2]^{2-}$) can form the most stable complex with Fe^{2+} and/or Fe^{3+} . As a result, the tetrahedral complex $[\text{Fe}(\text{C}_2\text{H}_4\text{O}_2)_2]^-$ with the ligand $[\text{C}_2\text{H}_4\text{O}_2]^{2-}$ through O-donor chelating with Fe^{3+} was found to be the most probable and stable complex. However, the ethaline solvent did not deliver adequate Fe extraction compared to commonly used reagents/solvents like mineral acids, to fully break down pyrite and expose any encapsulated gold.

1. Introduction

Finely disseminated gold enclosed in sulfidic minerals (known as refractory ore) is typified by relatively low to moderate gold yield with the cyanidation process [46]. Among the sulfidic minerals, pyrite is a predominant host for gold, in which gold is occluded in its structure. Since the gold is locked inside the sulfidic host mineral, i.e. pyrite, it is necessary to break down the sulfidic matrix to expose the encapsulated gold [12]. This justifies the extra effort on the refractory gold ore and mine tailings to oxidise the impervious sulfidic mineral to obtain a permeable matrix to achieve satisfactory gold recovery through different methods and reagents [42].

The hydrometallurgical process involves principally the dissolution of minerals in an acidic and/or basic aqueous medium, followed by extracting the target metals [46]. Typically, industrial leaching solutions

contain water, acids (H_2SO_4 , HNO_3 , HCl), bases (NaOH , NH_4OH), complexing agents and oxidising agents such as H_2O_2 , Fe^{3+} , Cl_2 , HClO , to improve the rate of leaching [35]. Cyanide also has been used extensively for gold extraction for more than a century. However, besides being toxic and hazardous, in the case of refractory ores, cyanide is unable to extract the enclosed gold from pyrite [41,60].

The main reasons for searching for an eco-friendly and efficient substitute for cyanide and some other acidic and/or basic lixivants arise from the environmental, safety, and health concerns posed by their toxicity [19,60]. However, it is challenging to find an alternative reagent to compete with these powerful reagents to improve gold extraction from sulfidic refractory ores/mine tailings. A prospective reagent to break down the sulfidic structure of the host mineral to expose the enclosed gold and ultimately extract it, should fulfil some important criteria, such as being effective, relatively inexpensive,

* Corresponding author.

E-mail address: 1630835@students.wits.ac.za (S. Teimouri).

<https://doi.org/10.1016/j.molliq.2023.123468>

Received 29 August 2023; Received in revised form 27 October 2023; Accepted 30 October 2023

Available online 7 November 2023

0167-7322/© 2023 The Author(s). Published by Elsevier B.V. This is an open access article under the CC BY-NC-ND license (<http://creativecommons.org/licenses/by-nc-nd/4.0/>).

environmentally benign (non-toxic), and compatible with sulfidic refractory gold ores/mine tailings [16,14].

The rising of novel solvents started back in 1914 when Paul Walden discovered the first ionic liquid (IL), ethylammonium nitrate ($[\text{C}_2\text{H}_5\text{NH}_3]^+[\text{NO}_3]^-$) with a melting point of 12 °C. However, it was only since 2000, that ionic liquids (ILs) started to gain prominence as emerging solvents among researchers in different domains, especially in the extraction and recovery of valuable and critical metals [28,52]. ILs belong to the melton salt family comprising a large organic cation and inorganic or organic anions of different sizes. They are in a liquid state at temperatures lower than 100 °C or even room temperature, because the size difference between the cation and anion results in low lattice energy and a low melting point [45,36].

Recently, the green features of some ILs have been contested, mainly due to their poor biodegradability [24]. Their large-scale application may also be restricted due to being expensive solvents [40]. Meanwhile, Abbott et al. [3] discovered a new class of solvents entitled “deep eutectic solvents (DESs)” as an analogue of ILs. The first DES was formed by mixing choline chloride (ChCl) and urea at a molar ratio of (1:2), resulting in a substance that was liquid at room temperature with a melting point of 12 °C. In contrast, the melting points of the starting components ChCl and urea were 302 °C and 133 °C, respectively [44]. A DES typically contains two or three safe and relatively cheap components that have the capability of hydrogen bond interactions with each other, to make a eutectic mixture with a melting point lower than the constituting components. They are also known as low transition temperature mixtures (LTTMs) [2,40,18]. The reason for the considerable reduction in the melting point of a eutectic solvent compared to its pure starting components is due to charge delocalization that happens through hydrogen bond formation between the halide anion of the hydrogen bond acceptor (HBA) and the hydrogen bond donor (HBD) [26,20].

The most used component in reported DESs is ChCl ($[(\text{CH}_3)_3\text{NCH}_2\text{CH}_2\text{OH}]^+\text{Cl}^-$), which is a quaternary ammonium salt that is non-toxic, biodegradable, and comparatively cheap (compared to imidazolium and pyridinium cations in ILs). It is categorized as a provitamin and has been used as a nutrient substance in vitamin B, and animal food [40,44]. DESs, like ILs, can be designed for an intended purpose, since the physicochemical properties like melting point, viscosity, and conductivity of a DES can be altered by combining different halide salts (HBA) with various HBD in a different ratio to make a solvent with desired properties [40].

Usually, DESs have relatively high viscosities (>100 cP) at ambient conditions, which is attributed mainly to their extensive hydrogen bond network, electrostatic interactions, and Van der Waals forces between the components [20]. One way to decrease the viscosity of DESs is increasing temperature since it has a significant effect on reducing viscosity by increasing the mobility of species in DESs. Furthermore, adding water to a DES can decrease its viscosity to a large extent, depending on the amount of water used [27,20]. The reason why adding water to a DES can reduce its viscosity is due to the shifting of a great affinity for HBD to form H-bonding with chloride ions (in the case of the choline chloride-based DES) to the water molecules (HBD-water > HBD-Cl⁻), since water molecules have a higher polarity than other species, i.e. Cl⁻, in the system [61,15,22]. For instance, the viscosity of the ChCl/urea (1:2) mixture decreased from 527.3 (pure state) to 200.6 cP at 30 °C, with the addition of just 0.1 mol fraction of water to the ChCl/urea DES [13].

Therefore, DESs can be a potential alternative to traditional metal processing leachants/reagents, one that is environmentally benign with components that are commercially available and inexpensive [1]. DESs possess similar interesting physicochemical properties to ILs, but are cheaper, easier to make, biocompatible, and biodegradable [55,11]. There is increasing interest due to these remarkable properties of DESs as neoteric solvents [44] in various research fields like synthesis [8,57], catalysis [33,59], dissolution and extraction [51,37,54,34],

electrochemistry [29,40], desulfurization [23,21], CO₂ capture [53,5,38,25], and for water treatment/purification [6,47,32].

Abbott et al. [4] investigated the selective recovery of gold from gold concentrate ore through an electro-catalysis technique using DES called ethaline (mixture of ChCl and EG with a mole ratio of 1:2), with iodine (I₂) as an electro-catalyst oxidant. The gold concentrate ore mostly contains galena (PbS), pyrite (FeS₂), and chalcocopyrite (CuFeS₂), with quartz (SiO₂) and a small amount of gold in the form of electrum (a natural alloy of gold and silver). They observed that electrum, galena, and chalcocopyrite were soluble under oxidising conditions by iodine in a DES ethaline, whereas, pyrite was less soluble [4]. In other research, Abbott et al. [1] examined the electrochemical performance of pyrite in a DES ethaline. In a novel approach a pyrite-ethaline paste painted on a Pt flag as the working electrode was used to study the reduction-oxidation reactions. It was observed that the electrochemical dissolution of pyrite occurred in three consecutive steps, namely oxidative reactions, transferring electrons, followed by cathodic reactions. The CV scan detected two anodic peaks associated with the formation of Fe³⁺ and elemental sulfur (S⁰), along with three distinct cathodic peaks, one attributed to Fe³⁺/Fe²⁺ reduction, and the other two peaks related to sulfur reduction. Thus, refractory minerals such as pyrite can be dissolved to some extent in ethaline media via electrolysis [1].

Zhu et al. [62] studied a DES made of ChCl-urea-EG for zinc extraction from zinc oxide dust. They found that with a slurry concentration of 50 g/L, and a stirring speed of 600 rpm at 80 °C, the efficiency of zinc extraction was 85.2%. The kinetics of the dissolution process in the DES medium in a temperature range of 60–90 °C was diffusion-controlled with an activation energy of 32.1 kJ/mol. Vieira et al. [54] investigated phenolic compounds extraction from the leaves of a walnut tree (scientific name, *Juglans regia*) with ChCl-based DES as the HBA mixed with 15 different carboxylic acids as the HBD in the molar ratio of 1:2. The evaluation of the different carboxylic acids was assessed based on the number of carboxylic groups, the length of the alkyl chain, and additional hydroxyl and/or phenyl groups on the formed DES for high extraction efficiency. After extraction and analysis, it was determined that the two most effective DESs were the ones containing phenyl propionic acid and butyric acid, separately acting as the HBD. Then three independent variables (time, temperature and water content) in the two effective DESs were optimized by response surface methodology (RSM) using the design of experiments. The optimum condition was 180 min, 30 °C, and 49.3% water content resulting in 34.3 ± 0.2 mg/g dw (dry weight) and 33.7 ± 0.4 mg/g dw phenolic compounds extraction with phenyl propionic acid and butyric acid, respectively [54].

In research by Xu et al. [56], the application of metal-based DES was examined for extractive oxidation using peroxymonosulfate (HSO₅⁻) as the oxidant for the desulfurization of fuels. The metal-based DES was prepared by mixing cobalt chloride (CoCl₂), ChCl (HBA) and the HBD such as polyethylene glycol (PEG), glycerol (GL), ethylene glycol (EG), and propionic acid (PR). Among the four different HBDs, the combination of (CoCl₂-ChCl/2PEG) achieved almost 100% sulfur compound removal as the most effective with a fast reaction. The obtained optimum condition was 2 g of CoCl₂-ChCl/2PEG, 0.9 g of the oxidant, and 6 g of the studied oil with 500 ppm initial sulfur content, at 20 °C, for 60 min. Comparatively, the efficiency of the different HBDs used in the DES for desulfurization followed this order: PEG > PR > EG > GL. Interestingly, the studied DESs exhibited remarkable recycling and reutilizing performance, being used 6 times without a substantial decline in the desulfurization ability [56].

The desulfurization of fuels was also studied by Lee et al. [23] by evaluating the combination of tetraethyl ammonium bromide salts (C2–C8) as HBA and alkyl diols (C2–C5) as HBDs to prepare 18 different DESs. They have examined these DES for their efficiency in multiple aspects including sulfur removing, solubility with the studied oil, and cost-effectiveness. According to the results the DES prepared with tetraethyl ammonium bromide (TEAB) and 1,4-butanediol (1,4-BD) with a

1:4 M ratio were the most efficient, under experimental conditions of 1:1 DES/oil volume ratio, for 30 min at 25 °C, as well as being efficient for three consecutive uses. Generally, the longer the HBA alkyl chain, the more efficient the DES was for sulfur compound removal due to improvement in the hydrophobicity feature [56].

In this work, the feasibility of pyrite dissolution in a DES comprised of ChCl and EG, named "Ethaline" as a novel eco-friendly solvent was examined both experimentally and theoretically. The dissolution of pyrite was studied in ethaline with hydrogen peroxide oxidant by altering the pH of the ethaline solvent as one of the vital experimental factors, as well as the solid-to-liquid ratio. Ethaline containing ChCl and EG provides two ligands, i.e. Cl^- and $[\text{C}_2\text{H}_4\text{O}_2]^{2-}$ that can make complexes with $\text{Fe}^{2+/3+}$, hence destroying the pyrite structure. Therefore, to determine which of these two ligands can form the most probable complex with $\text{Fe}^{2+/3+}$, the reaction Gibbs free energy (ΔG) of the possible complexes was calculated through density functional theory (DFT). Moreover, the gap between the highest occupied molecular orbital (HOMO) and the lowest unoccupied molecular orbital (LUMO) of the proposed complexes was calculated. Typically, a low ΔG represents a high probability of a complex to form and a large gap between HOMO and LUMO indicates the stability of the formed complex. All calculations in DFT were performed using Gaussian 16, the B3LYP functional method in the gas phase and the PBEPBE Def2TZVP basis set. Ultimately the experimental results and the theoretical calculations were compared to draw a comprehensive conclusion. The results of this work make a further contribution to the field of pretreating refractory matrices (by breaking down pyrite) to improve gold recovery by using alternative solvents other than cyanide.

2. Experimental

2.1. Apparatuses and chemicals

The pyrite sample used in this work was analysed with XRD (Bruker, Karlsruhe, Germany) for its chemical composition. The leached solution was analysed by AAS (atomic absorption spectroscopy, Varian AA240, USA), to measure the content of extracted Fe. The samples in liquid form, ethylene glycol, and ethaline (before and after pyrite leaching), and also choline chloride (solid) were characterized with Fourier-transform infrared (FTIR) spectroscopy (Spectrum Two, Perkin Elmer, Ynysmaerdy, Pontyclun, UK), at room temperature over a range of 4000 to 400 cm^{-1} . The chemicals used in this research were choline chloride, and ethylene glycol, for synthesizing the deep eutectic solvent ethaline, hydrogen peroxide as the oxidant, hydrochloric acid, and sodium hydroxide for adjusting the pH. All of the chemicals were purchased from Merck.

2.2. Procedure

The ethaline solvent was synthesized through the heating-stirring method proposed by Abbott et al. [2] by mixing ChCl as the HBA with EG as the HBD in a molar ratio of (1:2.5). The molar ratio of (1:2.5) was selected over the more studied ratio of (1:2) since it will result in less viscous DES, favorable for extracting purposes. To synthesize ethaline, the calculated amount of both ChCl and EG were measured accurately, then mixed in a clean beaker and heated to 80 °C on a hot plate and stirred for 1 h to form a colorless uniform solvent. Fig. 1 illustrates the structure of ChCl and EG after being mixed and developing the hydrogen bond to make the ethaline solvent.

To determine the viability of Fe extraction as an indication of pyrite dissolution using ethaline and hydrogen peroxide, different pH values and solid-to-liquid (S/L) ratios were examined experimentally. Ethaline is stable in air and water (moisture) and can be used in experiments under atmospheric conditions [4]. The pyrite leaching experiment in the ethaline medium with hydrogen peroxide oxidant was carried out under atmospheric conditions in a 100 ml three-neck round bottom flask

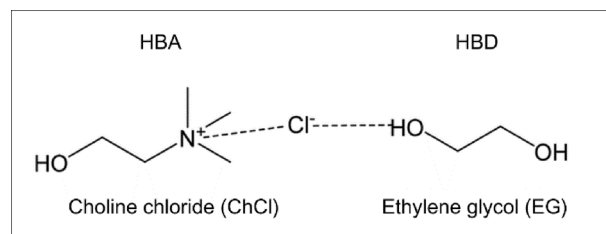


Fig. 1. Structure of ChCl and EG and the hydrogen bonding between them.

immersed in a water bath on top of a hot plate magnetic stirrer. The round bottom flask (leaching reactor) was connected to a water cooling condenser, the other neck holding the thermometer inside the leaching solution and the other one for taking sample at intervals. The mixing was done by a stirring bar inside the flask to provide a uniform pulp at 700 rpm, at a temperature of 65 °C. To follow the progress of the pyrite dissolution, 1 ml leached sample was taken from the reactor at time intervals of 0.5, 1, 1.5, 2, 3, 4, 5, and 6 h, and the same amount of ethaline with adjusted pH was added to the reactor to keep the ratio constant. Then the leached samples taken at intervals were diluted and analysed with AAS for Fe content. The experiments have been repeated and the average value was used to plot the graphs.

3. Results and discussion

3.1. Materials

The pyrite (FeS_2) sample used in this research was obtained from Mintek, South Africa. The X-ray diffraction (XRD) analysis was applied to check the main phase of the pyrite sample. Fig. 2 demonstrates the XRD pattern indicating the phase composition in which the pyrite phase with quartz as a small impurity was detected, proving the purity of the pyrite sample.

3.2. Experimental assessment

3.2.1. Effect of the Ethaline's pH

To evaluate the effect of the pH of the ethaline solvent on Fe extraction from the pyrite (FeS_2) sample, the pH of a 20 ml freshly synthesized ethaline (initial pH 6.2) was adjusted to pH of 4, 6, 8, 10, 11, and 12, and then added to the reactor. Once the temperature reached 65 °C, 1 g of well-mixed representative pyrite sample was added to the heated ethaline to make the S/L ratio of 1/20. A total volume of 2 ml hydrogen peroxide oxidant was also added in small amounts in intervals

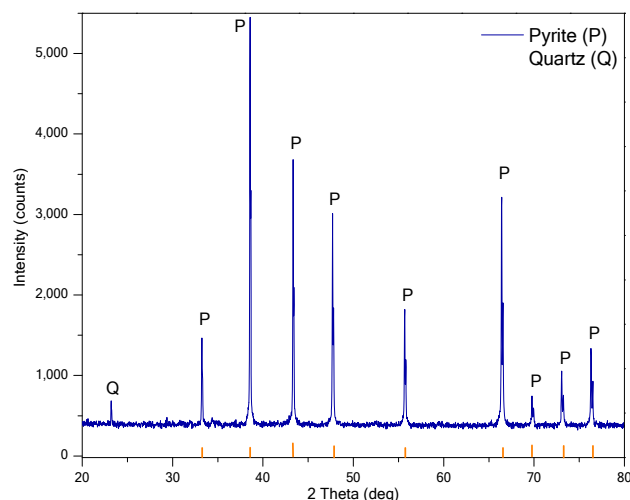
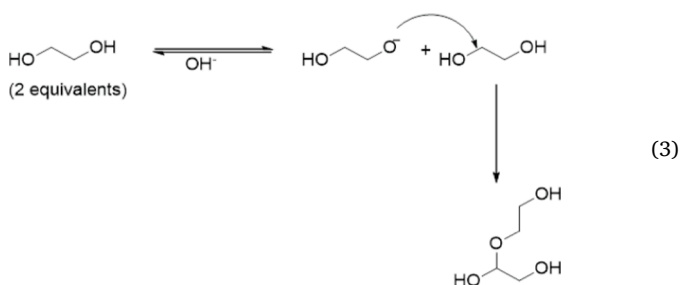
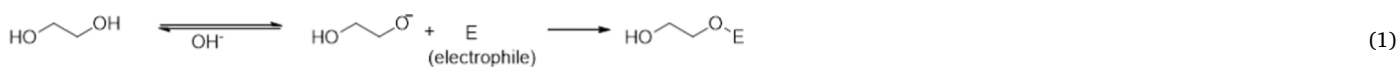


Fig. 2. The XRD pattern of the pyrite sample.

to have oxidant throughout the process. Typically, the chemical potential of H^+ and OH^- in the solution determining the pH, as well as their effect and interactions with other components/molecules in the mixture have a vital role in the extraction process [39].

In ethaline, the EG (CH_2OH-CH_2OH) component with two hydroxyl groups at each end of its structure can deprotonate to $(^-OCH_2-CH_2O^-)$ or $[C_2H_4O_2]^{2-}$ at basic pH as illustrated in reaction (1) [7,58]. Changing the pH in the basic range from 8 to 12 showed that pH 8 was the best for extracting Fe in the ethaline medium. The reason could be that at higher basic pH values the EG with the carbonyl functional group (electrophile), can shift to other structures based on reactions (2) and (3) [7,58]. Thus, increasing the pH to 12 had a reverse effect on Fe extraction and reduced it from 23.6% at pH 8 to 13.8% at pH 12 (Fig. 3).



Acidic pH 4 and 6 (the natural pH of synthesized ethaline) were also evaluated for Fe extraction as the indication of pyrite dissolution. The results show that Fe extraction takes place at acidic pH (6 and 4), but in smaller amounts than at pH 8, with 20.6% Fe extraction at pH 6 and 18.2% at pH 4 (Fig. 3). The more acidic the ethaline solution, the more H^+ ions are presented in the mixture, hence reducing the chance for deprotonation of EG [CH_2OH-CH_2OH] to $[C_2H_4O_2]^{2-}$, which is a

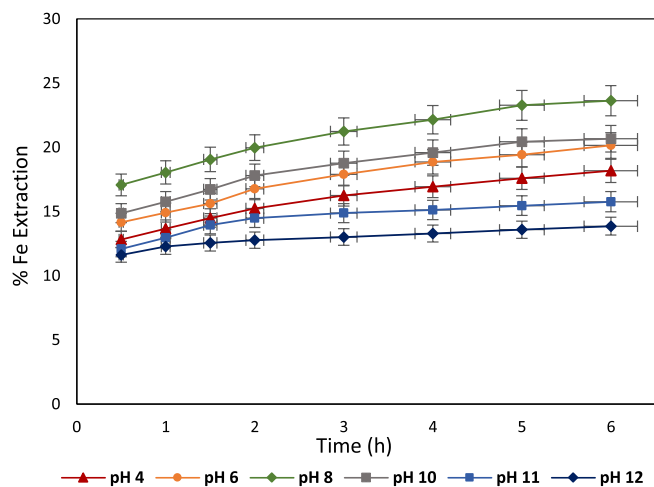


Fig. 3. Effect of the ethaline pH on Fe extraction. Operational conditions: 20 ml ethaline with 2 ml hydrogen peroxide, solid-to-liquid ratio 1/20, stirring speed 700 rpm, at 65 °C, for 6 h leaching time.

favourable ligand to form complexes with Fe. That could be the reason, the Fe extraction decreased at acidic pH.

3.2.2. Effect of solid-to-liquid ratio

The effect of solid-to-liquid (S/L) ratio on pyrite dissolution using ethaline as solvent was examined under the following experimental conditions: 20 ml ethaline (pH = 8), 2 ml hydrogen peroxide oxidant, and stirring speed of 700 rpm at 65 °C for 6 h. The predetermined amount of pyrite was added to the preheated ethaline to prepare the different solid-to-liquid ratios. As the results displayed in Fig. 4, by increasing the amount of solids in the solution to amend the S/L ratio of 1/10, the Fe extraction decreased slightly to 22.5%. This could be due to more solids creating more resistance in mass transfer, hence less

mobility, and alternatively, not enough leaching solution available per unit mass of solid (pyrite) [48,30]. Likewise, decreasing the amount of solid to the ratio of 1/25, also reduced the efficiency of Fe extraction (18%), since less solid (pyrite containing Fe) is present in the ethaline solution for extraction [49]. Therefore, in this system, the S/L ratio of 1/20 was the optimum with the right amount of solid, resulting in 23.6% Fe extraction.

3.2.3. Comparing nitric acid and ethaline

In a previous study by Teimouri et al. [50], pyrite dissolution in a nitric acid (HNO_3) solution was investigated. HNO_3 is an oxidising acid capable of breaking down sulfidic minerals, particularly pyrite. Comparing the results (Fig. 5) indicate that even a low concentration of HNO_3 solution of 1 M, with a shorter leaching time (2 h), leads to more Fe extraction of 44.6% (at 65 °C, S/L ratio 1/20, for 2 h), compared to ethaline leaching (pH = 8, at 65 °C, S/L ratio 1/20, for 6 h leaching) which only attained 23.6% Fe extraction. Although the ethaline DES is inexpensive, eco-friendly, and biodegradable, it was not sufficiently efficient to fully break down pyrite to expose enclosed gold to improve its yield.

3.2.4. Fourier-transform infrared (FTIR) spectroscopy

To evaluate the interaction between ChCl and EG making the ethaline solvent, FTIR was employed in the range of 4000–400 cm^{-1} by

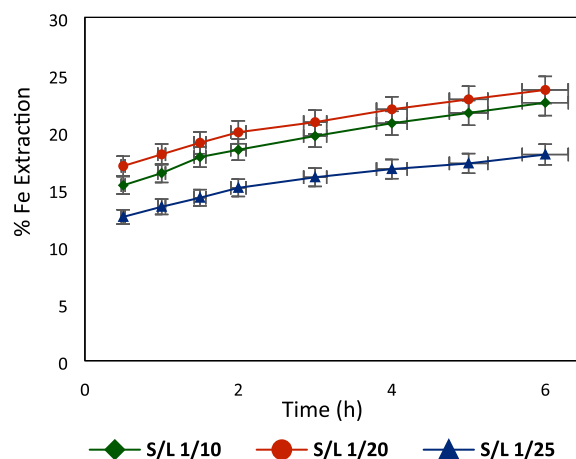


Fig. 4. Effect of the solid-to-liquid ratio on Fe extraction. Operational conditions: 20 ml ethaline, pH 8, stirring speed 700 rpm, at 65 °C, for 6 h leaching.

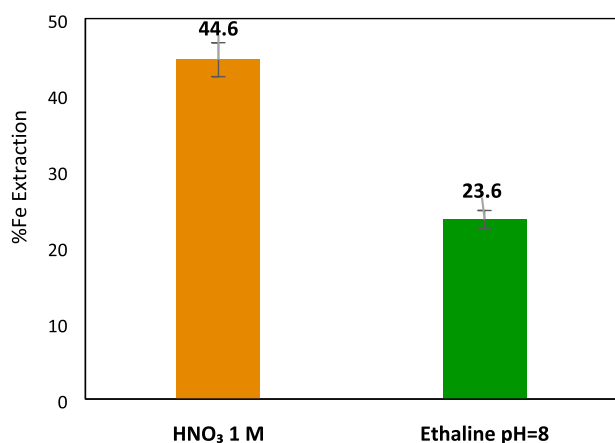


Fig. 5. Comparison of pyrite dissolution in 1 M HNO₃ (at 65 °C, S/L ratio 1/20, for 2 h leaching) and ethaline (pH = 8, at 65 °C, S/L ratio 1/20, for 6 h leaching).

measuring the spectra for (a) ChCl, (b) EG, (c) the synthesized ethaline (ChCl:EG), and (d) the ethaline after extracting Fe from pyrite (Fig. 6). From the synthesized ethaline spectrum, one can observe that it is a combination of the two spectra of ChCl and EG with slight changes, typically in a wavenumber shift indicating the interaction of the functional groups to develop hydrogen bonding to make the ethaline. The spectrum for ethaline shows vibrational bands at 3308 cm⁻¹ and 573 cm⁻¹ associated with stretching and bending of hydroxyl groups (O—H), respectively. The vibrational band at 3029 cm⁻¹ was attributed to C—H stretching, followed by a double peak (hybridized bending) at 2938 cm⁻¹ and 2875 cm⁻¹, which is ascribed to C—H₂ (sp³) stretching. The vibrational (peak) at 1481 cm⁻¹ is related to C—H₂ stretching of an alkyl

group. The vibrational peaks situated at 1206 cm⁻¹, 1137 cm⁻¹, 1085 cm⁻¹, 1037 cm⁻¹, and 882 cm⁻¹ till 573 cm⁻¹ are associated with C—C—O asymmetric stretching and C—O stretching [9,43,17].

The EG and ethaline spectra display similar vibrational patterns, except that the ethaline spectrum shows a weak and strong peak at 3029 cm⁻¹ and 954 cm⁻¹, respectively. The former (3029 cm⁻¹) is derived from the C—H stretching from ChCl, and the latter (954 cm⁻¹) is a characteristic ammonium (C—N) peak in the ethaline [43,17]. Comparing the ethaline solvent before and after leaching also shows that the vibrational stretching has a slight red shift (i.e. the O—H stretching shift from 3308 cm⁻¹ to 3303 cm⁻¹), indicating the engagement of the solvent with pyrite leaching. Interestingly, on the spectra of ethaline after being used for Fe extraction, a double peak at 1715 cm⁻¹ and 1643 cm⁻¹ appeared which can be related to Fe—O—C bound. This observation can indicate that the EG in the form of C₂H₄O₂²⁻ as a ligand in the solution forms complexes with Fe originating from pyrite.

3.2.5. Solid analysis: Scanning electron microscopy (SEM)

Fig. 7 shows scanning electron microscopy (SEM) images of the pyrite sample before and after leaching with ethaline solution (pH = 8, at 65 °C, S/L ratio 1/20, for 6 h leaching). As can be seen from the SEM image, before leaching the surface of the pyrite particles (FeS₂) looks smooth with few defects. However, after leaching in ethaline media, the morphology has changed to some extent as the surface of the pyrite particles looks rough and shows some defects. In addition, the surface of the pyrite grain was partially covered with agglomerated amorphous species, which could be sulfur. Fig. 8, demonstrates the scanning electron microscopy and energy dispersive X-ray spectroscopy (SEM-EDS) of pyrite before leaching detecting 51.2% and 47.7% (wt.%) of S and Fe, respectively approving the grain is certainly pyrite. Furthermore, on the residue, the formed agglomerated amorphous species on the surface of the pyrite grains were inspected with EDS and identified as sulphur

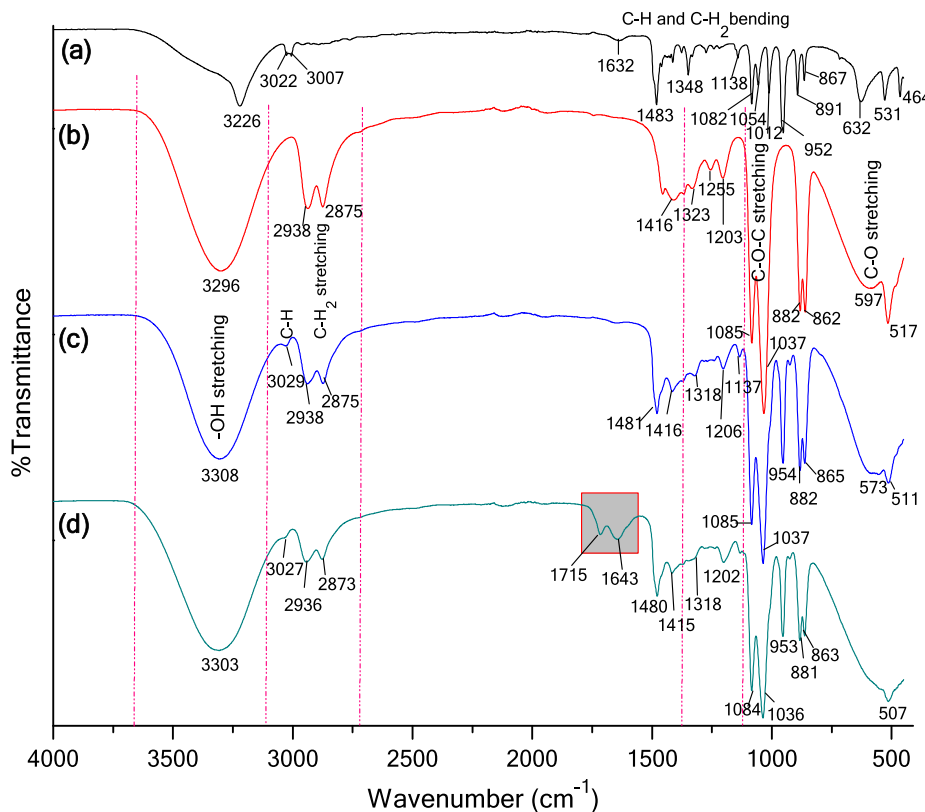


Fig. 6. FTIR spectra for (a) ChCl, (b) EG, (c) the synthesized ethaline (ChCl:EG), and (d) the ethaline after leaching pyrite.

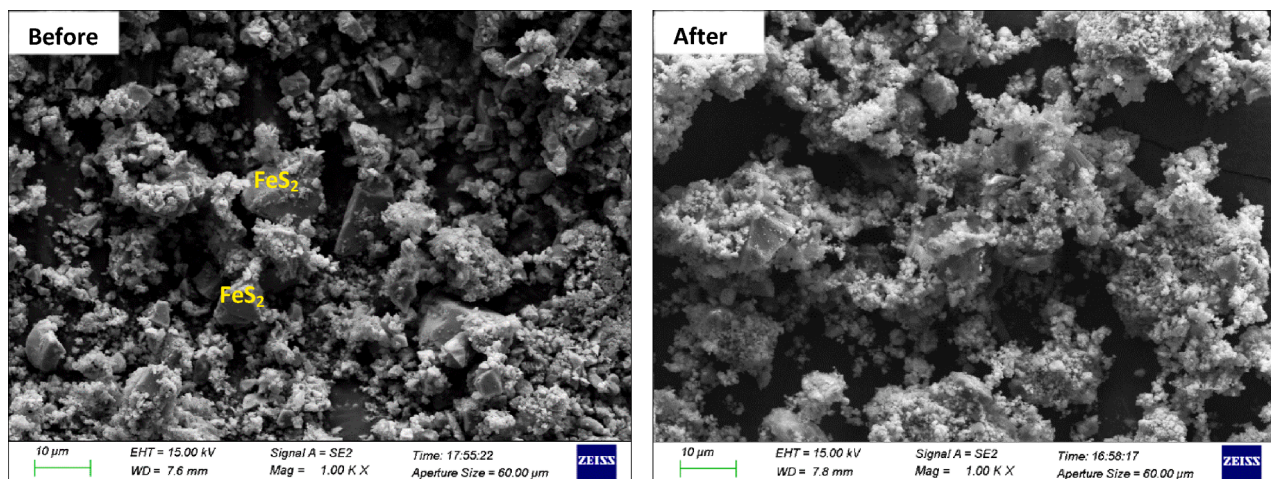


Fig. 7. SEM image of pyrite before and after leaching with DES ethaline (pH = 8, at 65 °C, S/L ratio 1/20, for 6 h leaching).

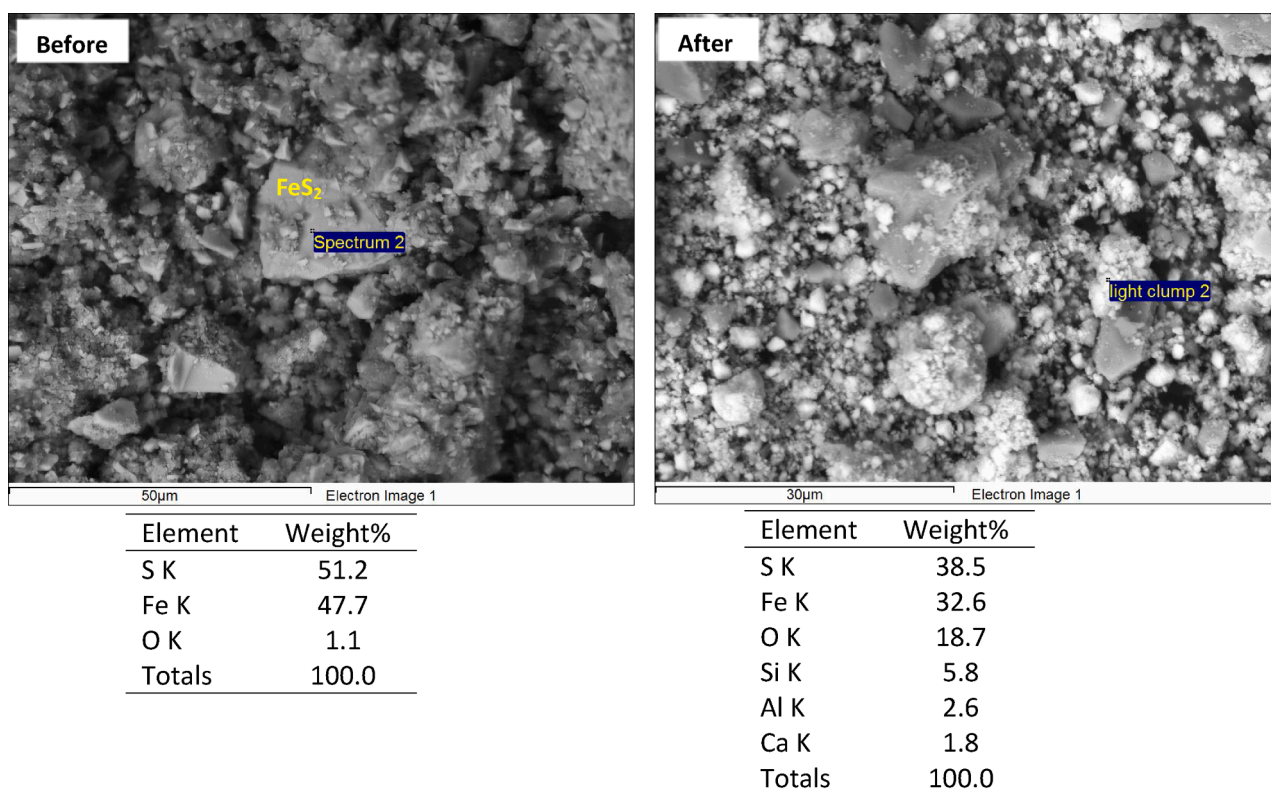


Fig. 8. SEM image and EDS results of the pyrite sample before and after leaching with DES ethaline.

species with 38.5% (wt.%) S. Moreover, the amount of Fe on the residue decreased to 32.6% (wt.%) after leaching with DES ethaline (pH = 8, at 65 °C) for 6 h, which could be due to pyrite dissolution.

3.3. Theoretical part: Density functional theory (DFT)

Density functional theory (DFT), based on the Kohn-Sham equation, was employed in this research to get a better perspective of the ligand–metal complexation, the shape of complexes and their stability [31]. The ethaline solvent has two ligands in its structure, EG in the form of $(C_2H_4O_2)^{2-}$ and Cl^- . To theoretically determine which of these two ligands most likely makes the most stable complex with Fe, DFT evaluation was applied. The possible reactions (4–11) resulting in a different complex format (i.e. tetrahedral, and octahedral), which can occur for

Fe^{2+} and Fe^{3+} with $[C_2H_4O_2]^{2-}$, and Cl^- are given as follows.

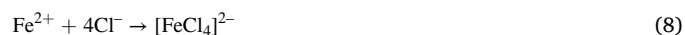
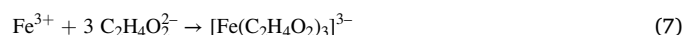
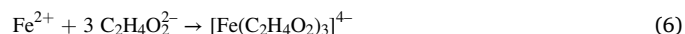
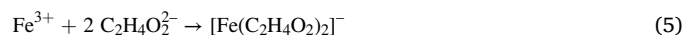
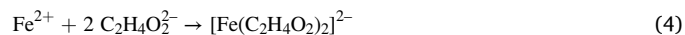


Table 1

The examined and the best multiplicity for each complex, including the ions.

Complex/Ion	Examined Multiplicities	Lowest Energy Multiplicity
$[\text{Fe}(\text{C}_2\text{H}_4\text{O}_2)_2]^{2-} (\text{Fe}^{2+})$	1, 3, 5	3
$[\text{Fe}(\text{C}_2\text{H}_4\text{O}_2)_2]^- (\text{Fe}^{3+})$	2, 4, 6	4
$[\text{Fe}(\text{C}_2\text{H}_4\text{O}_2)_3]^{4-} (\text{Fe}^{2+})$	1, 3, 5	5
$[\text{Fe}(\text{C}_2\text{H}_4\text{O}_2)_3]^{3-} (\text{Fe}^{3+})$	2, 4, 6	6
$[\text{FeCl}_4]^{2-} (\text{Fe}^{2+})$	1, 3, 5	5
$[\text{FeCl}_4]^- (\text{Fe}^{3+})$	2, 4, 6	4
$[\text{FeCl}_6]^{4-} (\text{Fe}^{2+})$	1, 3, 5	5
$[\text{FeCl}_6]^{3-} (\text{Fe}^{3+})$	2, 4, 6	6
$[\text{Fe}^{2+}]$	1, 3, 5	5
$[\text{Fe}^{3+}]$	2, 4, 6	6
$[\text{C}_2\text{H}_4\text{O}_2]^{2-}$	1, 3, 5	1
$[\text{Cl}]^-$	1, 3, 5	1

It should be mentioned that the different multiplicities, specifying a low spin and high spin, for both Fe^{2+} and the Fe^{2+} -complexes (1, 3, and 5) as well as Fe^{3+} and the Fe^{3+} -complexes (2, 4, and 6), were examined.

The multiplicity that leads to the lowest calculated energy for the formed complexes are listed in Table 1.

The reactions (4–11) were used to calculate the ΔG of each reaction which indicates the possibility of the formation of proposed complexes [10]. The calculation of ΔG for reaction (9), forming $[\text{FeCl}_4]^-$ (product), with Fe^{3+} and Cl^- (reactants), is written as an example:

$$\Delta G (\text{reaction 9}) = \Sigma \Delta G (\text{products}) - \Sigma \Delta G (\text{reactants}) = G ([\text{FeCl}_4]^-) - [G (\text{Fe}^{3+}) + G (4\text{Cl}^-)]$$

$$\Delta G (\text{reaction 9}) = -84463.42 - (-34324.26 + (4 \times -12520.06)) = -58.9 \text{ eV.}$$

The gap between HOMO and LUMO which indicates the stability of each complex was also calculated. The HOMO and LUMO structure of the complexes of Fe^{2+} and Fe^{3+} with each ligand $[\text{C}_2\text{H}_4\text{O}_2]^{2-}$ and $[\text{Cl}^-]$ provided by the ethaline solvent are depicted in Fig. 9.

Table 2 summarized the obtained results for ΔG , and the HOMO–LUMO gap for the different complexes for Fe^{2+} and Fe^{3+} with each ligand $[\text{C}_2\text{H}_4\text{O}_2]^{2-}$ and $[\text{Cl}^-]$. Typically, the most probable and stable complex is the one with the lowest ΔG and a large HOMO–LUMO gap

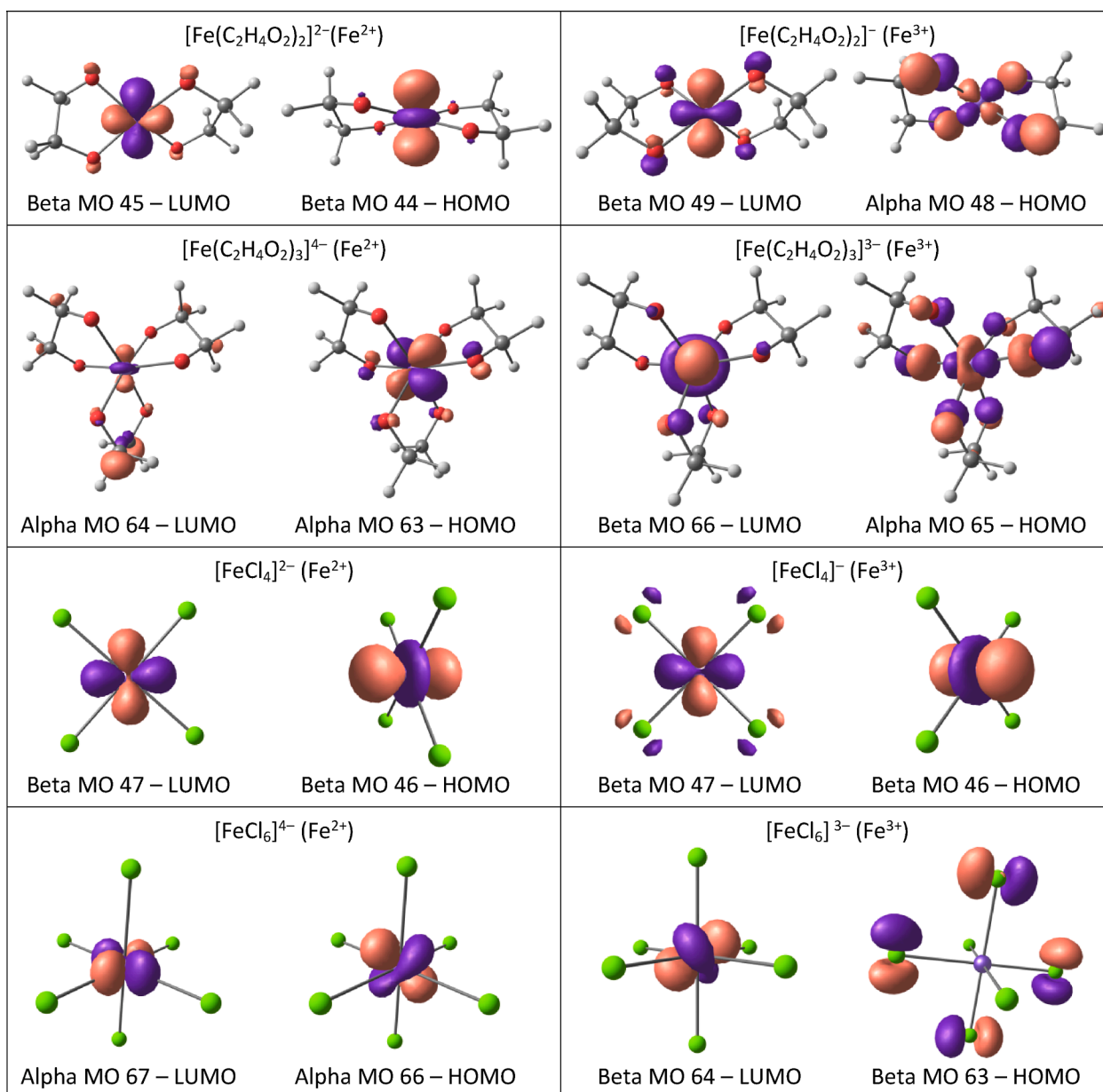
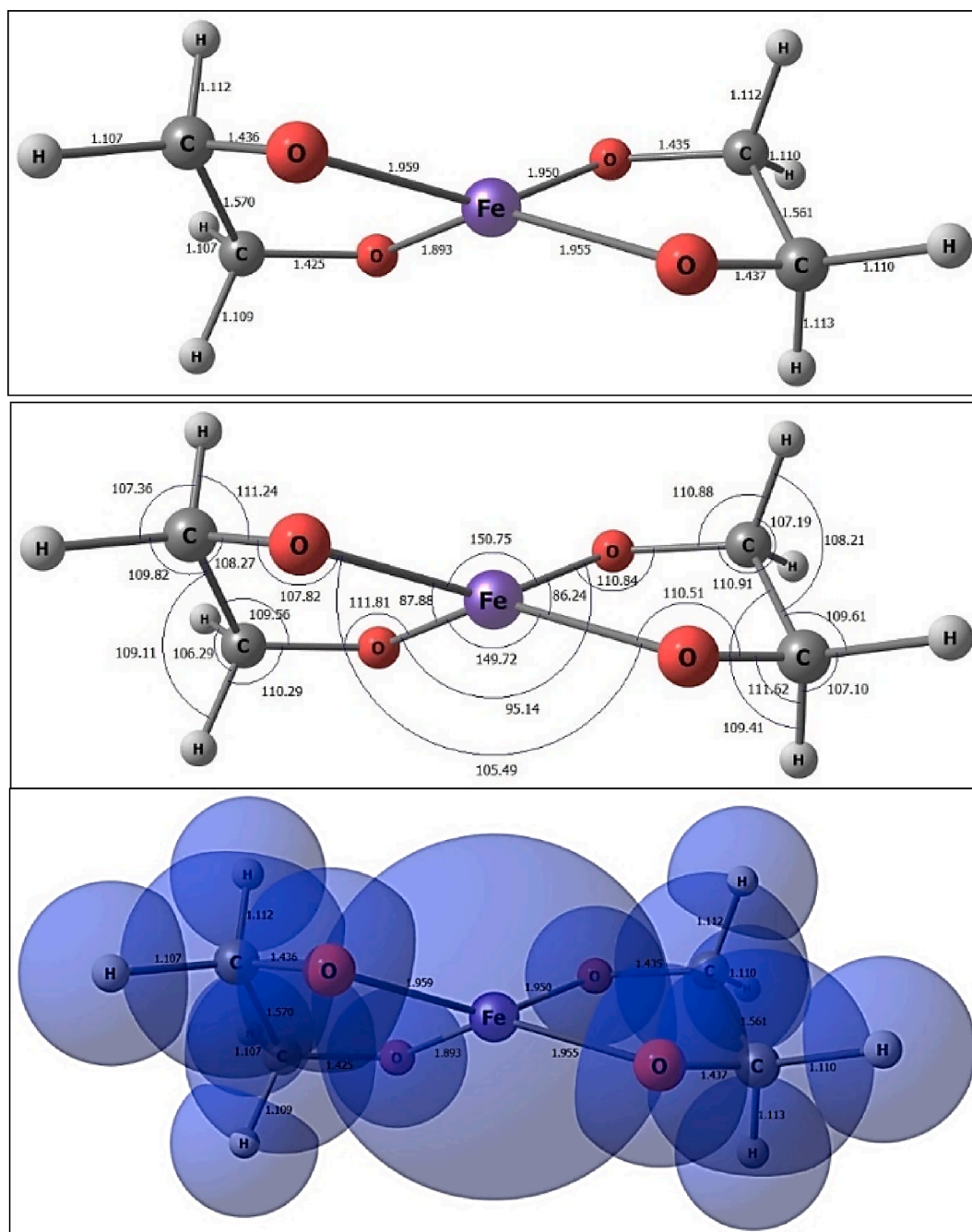


Fig. 9. The LUMO and HOMO of the complexes of Fe^{2+} and Fe^{3+} with ligands $[\text{C}_2\text{H}_4\text{O}_2]^{2-}$ and $[\text{Cl}^-]$.

Table 2The complexes of $[\text{C}_2\text{H}_4\text{O}_2]^{2-}$, and Cl^- with Fe^{2+} and Fe^{3+} , ΔG of the formation reaction, and HOMO–LUMO gap.

Fe complex	Fe oxidation state	Complex shape	ΔG (eV)	LUMO–HOMO gap (eV)
$[\text{Fe}(\text{C}_2\text{H}_4\text{O}_2)_2]^{2-}$	Fe^{2+}	Tetrahedral	– 34.3	0.89
$[\text{Fe}(\text{C}_2\text{H}_4\text{O}_2)_2]^-$	Fe^{3+}	<u>Tetrahedral</u>	<u>– 71.5</u>	<u>1.3</u>
$[\text{Fe}(\text{C}_2\text{H}_4\text{O}_2)_3]^{4-}$	Fe^{2+}	Octahedral	– 23.7	0.31
$[\text{Fe}(\text{C}_2\text{H}_4\text{O}_2)_3]^{3-}$	Fe^{3+}	Octahedral	– 34.3	1.2
$[\text{FeCl}_4]^{2-}$	Fe^{2+}	Tetrahedral	– 25.02	0.84
$[\text{FeCl}_4]^-$	Fe^{3+}	Tetrahedral	– 58.9	0.53
$[\text{FeCl}_6]^{4-}$	Fe^{2+}	Octahedral	– 7.9	0.55
$[\text{FeCl}_6]^{3-}$	Fe^{3+}	Octahedral	– 48.1	1.1

**Fig. 10.** The most probable and stable complex $[\text{Fe}(\text{C}_2\text{H}_4\text{O}_2)_2]^-$ in geometry-optimized form, with labelled angles, the length of each bond, and the Van-Deer-Waal sphere.

[31,10]. The calculated ΔG of the reactions forming the proposed complexes were all negative, indicating spontaneous formation. Among them the tetrahedral complex of $[\text{C}_2\text{H}_4\text{O}_2]^{2-}$ O-donor chelating ligand with Fe^{3+} in the form of $[\text{Fe}(\text{C}_2\text{H}_4\text{O}_2)_2]^-$ had the lowest ΔG , and the largest HOMO–LUMO gap, signifying the most likely complex to form. This was also in agreement with FTIR identifying the Fe–O–C bonding as part of this complex, $[\text{Fe}(\text{C}_2\text{H}_4\text{O}_2)_2]^-$.

The geometry-optimized form of $[\text{Fe}(\text{C}_2\text{H}_4\text{O}_2)_2]^-$ complex with the labelled length of each bond, angles, and the Van-Der-Waal sphere is presented in Fig. 10.

Although there was research by the Abbott group on pyrite in DES ethaline, the emphasis of their research was on the viability of dissolution through the electrolysis method with iodine as the oxidant [4]. The other research focused on pyrite-ethaline paste on the Pt electrode as a novel electrochemical method to determine the dissolution mechanism [1]. Hence, a direct comparison is not possible, since this work investigates a conventional leaching method for pyrite dissolution in ethaline media with hydrogen peroxide oxidant.

4. Conclusions

The viability of pyrite dissolution in ethaline media with hydrogen peroxide oxidant was examined both experimentally and theoretically. The evaluation at various pH values (4, 6, 8, 10, 11, 12) and solid-to-liquid ratios (1/10, 1/20, 1/25), were conducted with the aim of Fe extraction as an indication of any pyrite dissolution. DFT calculations were employed to theoretically determine the most likely complex to form. The following can be concluded after this study:

- At pH 8 and the S/L ratio of 1/20, the Fe extraction yield was 23.6%, which is lower than what was achieved with a 1 M nitric acid solution yielding 46.3% Fe extraction.
- DFT calculations reveal that the tetrahedral complex of $[\text{C}_2\text{H}_4\text{O}_2]^{2-}$ via an O-donor chelating ligand with Fe^{3+} in the form of $[\text{Fe}(\text{C}_2\text{H}_4\text{O}_2)_2]^-$ had the lowest ΔG , and the largest HOMO–LUMO gap which indicates the most probably and stable complex to form.
- The FTIR spectrometry indicates a double peak at 1715 cm^{-1} and 1643 cm^{-1} , which can be related to Fe–O–C bonding, which only appeared in the spectrum of the ethaline after leaching pyrite, thus proving the formation of the complex between $[\text{C}_2\text{H}_4\text{O}_2]^{2-}$ and Fe.

Ethaline DES is however not sufficiently efficient in breaking down pyrite to fully dissolve it to expose any encapsulated gold to improve the yield. Hence, more research is required to be done with DESs on metal extraction to find an effective eco-friendly method that can compete with traditional reagents.

CRedit authorship contribution statement

Samaneh Teimouri: Investigation, Methodology, Formal analysis, Software, Project administration, Data curation, Visualization, Writing – original draft. **Johannes Herman Potgieter:** Supervision, Funding acquisition, Writing – review & editing. **Caren Billing:** Supervision, Resources, Conceptualization, Data curation, Validation. **Jeanet Conradie:** Resources, Software, Conceptualization, Validation, Writing – review & editing.

Declaration of Competing Interest

The authors declare that they have no known competing financial interests or personal relationships that could have appeared to influence the work reported in this paper.

Data availability

The authors do not have permission to share data.

Acknowledgement

The NICIS CSIR Centre for High Performance Computing (CHPC, grant CHEM0947) of RSA is acknowledged for processing time. Sincere appreciation is expressed to Dr Alhadji Malloum for his guidance in DFT modelling.

Funding

This research was financially supported by DRDGOLD Ltd. in South Africa. The DFT modelling was done through a High-performance computer at the NICIS CSIR Centre for High Performance Computing (CHPC, grant CHEM0947) of RSA.

Appendix A. Supplementary material

Supplementary data to this article can be found online at <https://doi.org/10.1016/j.molliq.2023.123468>.

References

- [1] A.P. Abbott, A.Z.M. Al-Bassam, A. Goddard, R.C. Harris, G.R.T. Jenkin, F.J. Nisbet, M. Wieland, Dissolution of Pyrite and other Fe-S-As minerals using Deep Eutectic Solvents, *Green Chem.* 19 (9) (2017) 2225–2233.
- [2] A.P. Abbott, D. Boothby, G. Capper, D.L. Davies, R.K. Rasheed, Deep Eutectic Solvents Formed between Choline Chloride and Carboxylic Acids: Versatile Alternatives to Ionic Liquids, *J. Am. Chem. Soc.* 126 (9) (2004) 9142–9147.
- [3] A.P. Abbott, G. Capper, D.L. Davies, R.K. Rasheed, V. Tambyrajah, Novel solvent properties of choline chloride/urea mixtures, *Roy. Soc. Chem.* 2003 (2002) (2003) 70–71.
- [4] A.P. Abbott, R.C. Harris, F. Holyoak, G. Frisch, J. Hartley, G.R.T. Jenkin, Electrocatalytic recovery of elements from complex mixtures using deep eutectic solvents, *Green Chem.* 17 (4) (2015) 2172–2179.
- [5] I. Adeyemi, M.R.M. Abu-zahra, I. Alnashef, Experimental Study of the Solubility of CO_2 in Novel Amine Based Deep Eutectic Solvents, *Energy Procedia* 105 (2017) (2017) 1394–1400.
- [6] K. Aruchamy, R.N. Maalige, M.M. Halanur, A. Mahto, R. Nagaraj, D. Kalpana, D. Ghosh, D. Mondal, S.K. Nagaraj, Ultrafast synthesis of exfoliated manganese oxides in deep eutectic solvents for water purification and energy storage, *Chem. Eng. J.* 379 (2020) (2020) 1–10.
- [7] M. Calatayud, Ethylene glycol interaction on alkaline earth oxides: A periodic DFT study, *Catal. Today* 152 (1–4) (2010) 88–92.
- [8] D. Carriazo, M. Concepcion, L. Ferrer, F. Monte, Deep-eutectic solvents playing multiple roles in the synthesis of polymers and related materials, *Chem. Soc. Crit. Rev.* 41 (2012) (2012) 4996–5014.
- [9] N. Delgado-mellado, M. Larriba, P. Navarro, V. Rigual, M. Ayuso, J. García, F. Rodríguez, Thermal stability of choline chloride deep eutectic solvents by TGA/FTIR-ATR analysis, *J. Mol. Liq.* 260 (2018) (2018) 37–43.
- [10] H. Ferreira, M.M. Conradie, K.G. von Eschwege, J. Conradie, Electrochemical and DFT study of the reduction of substituted phenanthrolines, *Polyhedron* 122 (2017) (2017) 147–154.
- [11] C. Florindo, F. Lima, B.D. Ribeiro, I.M. Marrucho, ScienceDirect Deep eutectic solvents: overcoming 21st century challenges, *Curr. Opin. Green Sustainable Chem.* 18 (2019) (2018) 31–36.
- [12] G. Gao, D. Li, Y. Zhou, X. Sun, W. Sun, Kinetics of high-sulphur and high-arsenic refractory gold concentrate oxidation by dilute nitric acid under mild conditions, *Miner. Eng.* 22 (2) (2009) 111–115.
- [13] G. García, S. Aparicio, R. Ullah, M. Atilhan, Deep eutectic solvents: Physicochemical properties and gas separation applications, *Energy Fuel* 29 (4) (2015) 2616–2644.
- [14] M. Göknelma, A. Birich, S. Stopic, B. Friedrich, A Review on Alternative Gold Recovery Reagents to Cyanide, *J. Mater. Sci. Chem. Eng.* 4 (2016) (2016) 8–17.
- [15] O.S. Hammond, D.T. Bowron, K.J. Edler, The Effect of Water upon Deep Eutectic Solvent Nanostructure: An Unusual Transition from Ionic Mixture to Aqueous Solution, *Angew. Chem.* 129 (2017) (2017) 9914–9917.
- [16] G. Hilson, A.J. Monhemius, Alternatives to cyanide in the gold mining industry: what prospects for the future? *J. Clean. Prod.* 14 (12–13) (2006) 1158–1167.
- [17] S. Imteyaz, C.M. Suresh, T. Kausar, P.P. Ingole, Carbon dioxide capture and its electrochemical reduction study in deep eutectic solvent (DES) via experimental and molecular simulation approaches, *J. CO₂ Utiliz.* 68 (2023) (2023), 102349.
- [18] M. Jancheva, S. Grigorakis, S. Loupassaki, D.P. Makris, Optimised extraction of antioxidant polyphenols from *Satureja thymbra* using newly designed glycerol-based natural low-transition temperature mixtures (LTTMs), *J. Appl. Res. Med. Aromat. Plants* 6 (2017) (2017) 31–40.
- [19] E. Jaszczak, Ż. Polkowska, S. Narkowicz, J. Namieśnik, Cyanides in the environment — analysis — problems and challenges, *Environ. Sci. Pollut. Res.* 24 (2017) (2017) 15929–15948.
- [20] P. Kalhor, K. Ghandi, Deep Eutectic Solvents for Pretreatment, Extraction, and Catalysis of Biomass and Food Waste, *Molecules* 24 (4012) (2019) 1–37.

- [21] N. Khan, V.C. Srivastava, Extractive desulfurization using ethylene glycol and glycerol-based deep eutectic solvents: engineering aspects and intensification using ultrasound, *Chem. Eng. Process. - Process Intensif.* 180 (2022) (2022), 108973.
- [22] P. Kumari, Shobhna, S. Kaur, H.K. Kashyap, Influence of Hydration on the Structure of Reline Deep Eutectic Solvent: A Molecular Dynamics Study, *Am. Chem. Soc.* 3 (11) (2018) 15246–15255.
- [23] H. Lee, S. Kang, Y. Jin, D. Jung, K. Park, K. Li, J. Lee, Systematic investigation of the extractive desulfurization of fuel using deep eutectic solvents from multifarious aspects, *Fuel* 264 (2020) (2020) 1–10.
- [24] X. Li, K.H. Row, Development of deep eutectic solvents applied in extraction and separation, *J. Sep. Sci.* 39 (18) (2016) 3505–3520.
- [25] Y. Liu, H. Yu, Y. Sun, S. Zeng, X. Zhang, Y. Nie, Screening Deep Eutectic Solvents for CO₂ Capture With COSMO-RS, *Front. Chem.* 8 (2020) (2020) 1–11.
- [26] Longo, Craveiro, Deep Eutectic Solvents as Unconventional Media for Multicomponent Reactions, *J. Braz. Chem. Soc.* 29 (10) (2018) 1999–2025.
- [27] C. Ma, A. Laaksonen, X. Ji, X. Lu, The peculiar effect of water on ionic liquids and deep eutectic solvents, *Roy. Soc. Chem.* 47 (2018) (2018) 8685–8720.
- [28] K.N. Marsh, J.A. Boxall, R. Lichtenthaler, Room temperature ionic liquids and their mixtures - A review, *Fluid Phase Equilib.* 219 (1) (2004) 93–98.
- [29] K. Miyazaki, T. Matsumiya, T. Abe, H. Kurata, T. Fukutsuka, K. Kojima, Z. Ogumi, Electrochemical oxidation of ethylene glycol on Pt-based catalysts in alkaline solutions and quantitative analysis of intermediate products, *Electrochim. Acta* 56 (22) (2011) 7610–7614.
- [30] Y. Moazzami, S.Z.S. Tonkaboni, M. Gharabaghi, Leaching Kinetics of Chalcopyrite Concentrate by Ionic Liquids, *Iran, J. Mater. Sci. Eng.* 19 (4) (2022) 1–14.
- [31] S. Mohammadnejad, J.L. Provis, J.S.J. van Deventer, Computational modelling of interactions between gold complexes and silicates, *Comput. Theor. Chem.* 1101 (2017) (2017) 113–121.
- [32] G. Moradi, M. Rahimi, S. Zinadini, M. Shamsipur, N. Babajani, Natural deep eutectic solvent modified nanofiltration membranes with superior antifouling properties for pharmaceutical wastewater treatment, *Chem. Eng. J.* 448 (2022) 137704.
- [33] R.M. Musale, S.R. Shukla, Deep eutectic solvent as effective catalyst for aminolysis of polyethylene terephthalate (PET) waste, *Int. J. Plast. Technol.* 20 (1) (2016) 106–120.
- [34] L. Nakhle, M. Kfoury, I. Mallard, D. Landy, H. Greige, Microextraction of bioactive compounds using deep eutectic solvents: a review, *Environ. Chem. Lett.* 19 (5) (2021) 3747–3759.
- [35] J. Niemczewska, R. Cierpiszewski, J. Szymanowski, Mass transfer of zinc (II) extraction from hydrochloric acid solution in the Lewis cell, *Desalination* 162 (2004) (2004) 169–177.
- [36] J. Park, Y. Jung, P. Kusumah, J. Lee, K. Kwon, C.K. Lee, Application of ionic liquids in hydrometallurgy, *Int. J. Mol. Sci.* 15 (9) (2014) 15320–15343.
- [37] X. Peng, M. Duan, X. Yao, Y. Zhang, C. Zhao, Green extraction of five target phenolic acids from *Lonicera japonica* Flos with deep eutectic solvent, *Sep. Purif. Technol.* 157 (2016) (2016) 249–257.
- [38] A. Pina, P. Ferrão, J. Fournier, B. Lacarrière, O.L. Corre, Development of Low-Cost Deep Eutectic Solvents for CO₂ Capture, *Energy Procedia* 142 (2017) (2017) 3320–3325.
- [39] V.S. Protsenko, A.A. Kityk, D.A. Shaiderov, F.I. Danilov, Effect of water content on physicochemical properties and electrochemical behavior of ionic liquids containing choline chloride, ethylene glycol and hydrated nickel chloride, *J. Mol. Liq.* 212 (2015) (2015) 716–722.
- [40] Z. Qinghua, D.O.V. Karine, R. Sébastien, J. François, Deep eutectic solvents: syntheses, properties and applications, *Chem. Soc. Rev.* 41 (2012) (2012) 7108–7146.
- [41] D.A. Rogozhnikov, A.A. Shoppert, O.A. Dizer, K.A. Karimov, R.E. Rusalev, Leaching kinetics of sulfides from refractory gold concentrates by nitric acid, *Metals* 9 (4) (2019) 1–15.
- [42] D. Rogozhnikov, K. Karimov, A. Shoppert, O. Dizer, S. Naboichenko, Kinetics and mechanism of arsenopyrite leaching in nitric acid solutions in the presence of pyrite and Fe (III) ions, *Hydrometall.* 199 (2020) (2021), 105525.
- [43] H. Sereshti, F. Karami, N. Nouri, A green dispersive liquid-liquid microextraction based on deep eutectic solvents doped with β -cyclodextrin: Application for determination of tetracyclines in water samples, *Microchem. J.* 163 (2021) (2021) 1–7.
- [44] E.L. Smith, A.P. Abbott, K.S. Ryder, Deep Eutectic Solvents (DESs) and Their Applications, *Chem. Rev.* 114 (21) (2014) 11060–11082.
- [45] S. Sowmiah, V. Srinivasadesikan, M.C. Tseng, Y.H. Chu, On the chemical stabilities of ionic liquids, *Molecules* 14 (9) (2009) 3780–3813.
- [46] S. Syed, Recovery of gold from secondary sources - A review, *Hydrometall.* 115–116 (2012) (2012) 30–51.
- [47] M. Taghizadeh, A. Taghizadeh, V. Vatanpour, M. Reza, Deep eutectic solvents in membrane science and technology: Fundamental, preparation, application, and future perspective, *Sep. Purif. Technol.* 258 (2021) (2021), 118015.
- [48] S. Teimouri, G. Mawire, J.H. Potgieter, G.S. Simate, L. van Dyk, M. Dworzanowski, 2020-a. Using experimental design and response surface methodology (RSM) to optimize gold extraction from refractory sulphidic gold tailings with ionic liquids, *J. Southern Afr. Instit. Min. Metall.* 120(7), 415–423.
- [49] S. Teimouri, J.H. Potgieter, G.S. Simate, L. Van Dyk, M. Dworzanowski, Oxidative leaching of refractory sulphidic gold tailings with an ionic liquid, *Miner. Eng.* 156 (2020), 106484.
- [50] S. Teimouri, J.H. Potgieter, L. van Dyk, C. Billing, The Kinetics of Pyrite Dissolution in Nitric Acid Solution, *Materials* 15 (12) (2022) 4181.
- [51] M. Tomašević, K. Kovac, M.C. Bubalo, C. Natka, Green extraction of grape skin phenolics by using deep eutectic solvents, *Food Chem.* 200 (2016) (2016) 159–166.
- [52] M.A. Topçu, A. Rusen, Effect of 1-butyl-3-methylimidazolium based ionic liquids with different anions on copper recovery from copper anode slime, *J. Eng. Res. Appl. Sci.* 9 (2020) (2020) 1630–1635.
- [53] T.J. Trivedi, J.H. Lee, H.J. Lee, Y.K. Jeong, J.W. Choi, Deep eutectic solvents as attractive media for CO₂ capture, *Green Chem.* 19 (2016) (2016) 2834–2842.
- [54] V. Vieira, M.A. Prieto, L. Barros, J.A.P. Coutinho, I.C.F.R. Ferreira, O. Ferreira, Enhanced extraction of phenolic compounds using choline chloride based deep eutectic solvents from *Juglans regia* L, *Ind. Crop. Prod.* 115 (2018) (2018) 261–271.
- [55] M. Vilková, P. Justyna, V. Andrich, The role of water in deep eutectic solvent-base extraction, *J. Mol. Liq.* 304 (2020) (2020) 1–7.
- [56] H. Xu, D. Zhang, F. Wu, X. Wei, J. Zhang, Deep desulfurization of fuels with cobalt chloride-choline chloride/polyethylene glycol metal deep eutectic solvents, *Fuel* 225 (2018) (2018) 104–110.
- [57] D. Yu, Z. Xue, T. Mu, Perspective Deep eutectic solvents as a green toolbox for synthesis, *Cell Reports Phys. Sci.* 3 (4) (2022), 100809.
- [58] H. Yue, Y. Zhao, J. Gong, Ethylene glycol: properties, synthesis, and applications, *Chem. Soc. Crit. Rev.* 41 (11) (2012) 4218–4244.
- [59] M.H. Zainal-abidin, M. Hayyan, A. Hayyan, New horizons in the extraction of bioactive compounds using deep eutectic solvents: A review, *Anal. Chim. Acta* 979 (2017) (2017) 1–23.
- [60] Y. Zhang, M. Cui, J. Wang, X. Liu, X. Lyu, A review of gold extraction using alternatives to cyanide: Focus on current status and future prospects of the novel eco-friendly synthetic gold lixivants, *Miner. Eng.* 176(2021), 1–11. 107336.
- [61] T. Zhekenov, N. Toksanbayev, Z. Kazakbayeva, D. Shah, Fluid Phase Equilibria Formation of type III Deep Eutectic Solvents and effect of water on their intermolecular interactions, *Fluid Phase Equilib.* 441 (2017) (2017) 43–48.
- [62] X. Zhu, C. Xu, J. Tang, Y. Hua, Selective recovery of zinc from zinc oxide dust using choline chloride based deep eutectic solvents, *Trans. Nonferrous Met. Soc. Chin.* 29 (10) (2019) 2222–2228.